ACCOUNTS
of chemical research

Liquid Exfoliation of Defect-Free Graphene

JONATHAN N COLEMAN*
School of Physics and CRANN, Trinity College Dublin, Dublin 2, Ireland

RECEIVED ON JANUARY 6, 2012

CONSPECTUS

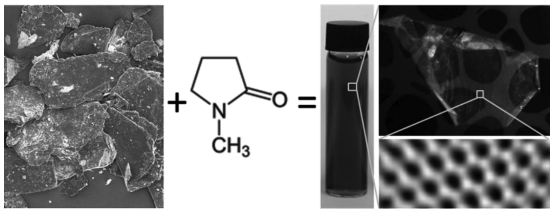

Due to its unprecedented physical properties, graphene has generated huge interest over the last 7 years. Graphene is generally fabricated in one of two ways: as very high quality sheets produced in limited quantities by micromechanical cleavage or vapor growth or as a rather defective, graphene-like material, graphene oxide, produced in large quantities. However, a growing number of applications would profit from the availability of a method to produce high-quality graphene in large quantities.

This Account describes recent work to develop such a processing route inspired by previous theoretical and experimental studies on the solvent dispersion of carbon nanotubes. That work had shown that nanotubes could be effectively dispersed in solvents whose surface energy matched that of the nanotubes. We describe the application of the same approach to the exfoliation of graphite to give graphene in a range of solvents. When graphite powder is exposed to ultrasonication in the presence of a suitable solvent, the powder fragments into nanosheets, which are stabilized against aggregation by the solvent. The enthalpy of mixing is minimized for solvents with surface energies close to that of graphene ($\sim$68 mJ/m^2). The exfoliated nanosheets are free of defects and oxides and can be produced in large quantities. Once solvent exfoliation is possible, the process can be optimized and the nanosheets can be separated by size. The use of surfactants can also stabilize exfoliated graphene in water, where the ζ potential of the surfactant-coated graphene nanosheets controls the dispersed concentration.

Liquid exfoliated graphene can be used for a range of applications: graphene dispersions as optical limiters, films of graphene flakes as transparent conductors or sensors, and exfoliated graphene as a mechanical reinforcement for polymer-based composites. Finally, we have extended this process to exfoliate other layered compounds such as BN and MoS_2. Such materials will be important in a range of applications from thermoelectrics to battery electrodes. This liquid exfoliation technique can be applied to a wide range of materials and has the potential to be scaled up into an industrial process. We believe the coming decade will see an explosion in the applications involving liquid exfoliated two-dimensional materials.

Introduction

Graphite has been used by man for thousands of years, originally for decorative purposes[1] but later in a range of applications from pencils to lining molds for cannon balls. While it had long been known that graphite had a stratified nature, the details of its layered structure were only revealed by Bernal in 1924 using X-ray crystallography.[2] We now know that graphite is a crystal consisting of stacked carbon monolayers, which are known individually as graphene.[3,4] A graphene sheet consists of an atomically thin array of sp^2-bonded carbon atoms organized in a planar hexagonal arrangement. Studied theoretically for many years,[5] thermodynamic arguments suggested that graphene could not exist as a free-standing entity.[6] Nevertheless, over the years a number of groups attempted to produce extremely thin graphitic lamellae.[7,8] This work culminated in 2004 with the discovery by Geim and Novosolov that individual sheets of graphene could be obtained by micromechanical cleavage of graphite.[9]

The novel electronic properties of graphene have been well documented.[4] In addition, graphene is ideal for a range of applications. For example, it is the strongest material known to man[10] and has been fabricated into large area transparent conductors.[11] Because of these exciting properties, a number of new methods of graphene production have

Published on the Web 03/20/2012 www.pubs.acs.org/accounts
10.1021/ar300009f

been developed such as annealing SiC substrates[12] or growth on metal supports.[13,14]

These methods for producing graphene have been very successful to date. However, it is likely that many future industrial applications of graphene will be in sectors such as large-area coatings or composite fillers, which require the production of graphene in very large quantities.[15] To this end, it is likely that liquid phase production methods will be required.[16]

Recently, a large number of papers have described the dispersion and exfoliation of graphene oxide (GO).[17] This material consists of graphene-like sheets chemically functionalized with groups such as hydroxyls and epoxides, which stabilize the sheets in water.[17] Graphene oxide has been an extremely successful material and has led to a string of advances.[18] However, the functionalization results in considerable disruption of the electronic structure of the graphene. In fact GO is an insulator rather than a semimetal and is conceptually different from graphene. While the functionalities can be removed by reduction, large defect populations remain, which continue to disrupt the electronic properties.[17] Thus, for a range of applications where pristine graphene is required, a noncovalent, solution-phase method to produce significant quantities of defect-free, unoxidized graphene would be extremely useful.

Liquid Exfoliation of Graphite To Give Graphene

Genesis. For a number of years before the popularization of graphene, a number of groups had studied the dispersion and exfoliation of carbon nanotubes in solvents.[19] In 2008, Bergin et al. combined experiment and thermodynamic modeling to show that the enthalpy of mixing of nanotubes per volume of solvent is given by[20,21]

$$\Delta H_{\mathrm{mix}}/V \approx 4(\sqrt{E_{S,\mathrm{NT}}} - \sqrt{E_{S,\mathrm{Sol}}})^2\phi/D \qquad (1)$$

where ϕ is the dispersed nanotube volume fraction, D is the dispersed nanotube (or bundle) diameter, and $E_{S,\mathrm{NT}}$ and $E_{S,\mathrm{Sol}}$ are the nanotube and solvent surface energies, respectively. This suggested successful solvents to be those with surface energy close to that of the nanotubes. Recently, we showed that the maximum dispersible concentration of rigid rods in solvents is given by[22]

$$\phi \approx K' \exp\left[-\frac{\bar{v}}{RT}\frac{\partial(\Delta H_{\mathrm{Mix}}/V)}{\partial\phi}\right] \qquad (2)$$

where K' is a constant and $\bar{v}$ is the molar volume of rods. Applying to nanotubes by inserting 1 into 2 gives

$$\phi \approx K' \exp\left[-\frac{\pi DL}{4E_{S,\mathrm{NT}}kT}(E_{S,\mathrm{NT}} - E_{S,\mathrm{Sol}})^2\right] \qquad (3)$$

where L is the mean nanotube length. This expression represents a Gaussian function when ϕ is plotted versus the solvent surface energy. Experimental data agree very well with this model confirming that nanotubes can be dispersed at relatively high concentrationonce the solvent and nanotube surface energies match.[20−22]

Exfoliation of Graphene in Solvents. Once the role of surface energy was known, it became immediately clear that because graphite has a surface energy similar to that of carbon nanotubes, it might be possible to exfoliate graphite to give graphene in certain solvents. To test this, we sonicated powdered graphite in a range of solvents using a low-power sonic bath.[23] We initially focused on solvents known to exfoliate nanotubes such as *N*-methyl-pyrrolidone (NMP) and dimethylformamide (DMF) (Figure 1A, inset). After centrifuging to remove any undispersed material, we measured the dispersed concentration using a combination of filtration, weighing, and absorption spectroscopy. We found that the dispersed concentration peaked for solvents with surface tensions close to 40 mJ/m^2, which is equivalent to surface energies of ∼70 mJ/m^2 (Figure 1A).[24] To understand this, we calculated the enthalpy of mixing for graphene flakes dispersed and exfoliated in solvents to be

$$\frac{\Delta H_{\mathrm{Mix}}}{V} \approx \frac{2}{T_{\mathrm{NS}}}\left(\sqrt{E_{S,S}} - \sqrt{E_{S,G}}\right)^2\phi_G \qquad (4)$$

where $E_{S,S}$ and $E_{S,G}$ are the solvent and graphene surface energy, respectively, T_{NS} is the nanosheet thickness, and ϕ_G is the dispersed graphene volume fraction. Assuming that we can use eq 2 to describe dispersed platelets, this predicts the dispersed graphene concentration ($C_G \propto \phi_G$) should be described by

$$C_G \propto \exp\left[-\frac{\pi {D_G}^2}{8E_{S,G}kT}(E_{S,S} - E_{S,G})^2\right] \qquad (5)$$

where D_G is the diameter of a graphene sheet (modeling it as a disk). Here we use the approximation $(x - a)^2 \approx 4a(\sqrt{x} - \sqrt{a})^2$ which is reasonably accurate so long as the full width at half maximum of the resulting Gaussian is less than about half the centre value. We find that this model fits the data extremely well (dashed line), suggesting a surface energy of graphene of ∼68 mJ/m^2. While a wide range of values have been reported for the surface energy of graphite, this is consistent with a recent value of 53 mJ/m^2, obtained from contact angle measurements.[25]

We analyzed the exfoliation state of the dispersed material in a number of solvents using transmission electron

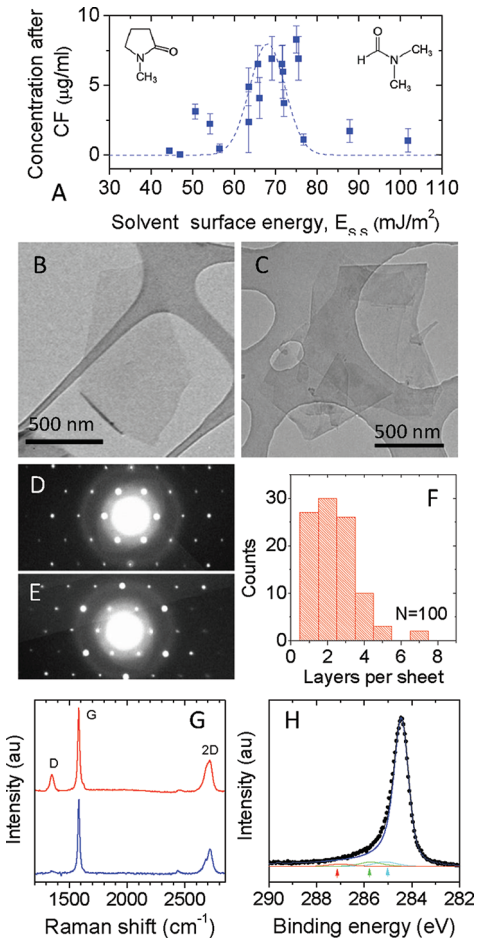

FIGURE 1. (A) Dispersed graphene concentration as a function of solvent surface energy. Insets show the structures of NMP (left) and DMF (right). (B, C) TEM images of graphene monolayer and multilayer respectively. (D, E) Electron diffraction patterns of graphene monolayer and multilayer, respectively. (F) Histogram showing the distribution of graphene layer thicknesses. (G) Raman spectra of (top) a small flake and (bottom) a larger flake. (H) C1s XPS spectrum of a thin film of graphene flakes. The contributions marked by arrows are due to the solvent.

microscopy. We found large quantities of two-dimensional objects, which appeared from careful examination of their edges[26] to be either monolayers (Figure 1B) or multilayers (Figure 1C). We can definitively identify the presence of monolayers by electron diffraction.[27] Shown in Figure 1D,E are electron diffraction patterns taken from what appear to be a graphene monolayer and a graphene bilayer, respectively. Computational studies have shown that the inner set of spots is more intense for monolayers and vice versa for multilayer graphene.[28] This is exactly what is found here, confirming our visible identification. Using a combination of electron diffraction and inspection, we can estimate the number of monolayers in each flake observed by TEM. As shown in Figure 1F, we found approximately 25% monolayers with the vast majority of flakes having <5 layers.[23]

While it is clear that graphite can be exfoliated in solvents to give monolayer and few layer graphene, it is not yet clear whether the graphene is pristine. To test this, we performed extensive Raman characterization of our exfoliated material.[23] Typically we observe spectra such as the upper one in Figure 1G, with a well-defined D band and a broad 2D band, characteristic of few layer flakes.[29] However, a D band around 1300 cm^{-1} is also observed, indicative of defects. It is worth noting that for flakes in the size range here, the edges will contribute to the spectrum, appearing as defects.[29] To test this, we identified a flake with dimensions significantly larger than the laser spot. Its spectrum is the lower one in Figure 1G and clearly displays no D band. Measurements such as these have clearly demonstrated that the flakes produced using solvent exfoliation are relatively defect-free. It is also important to confirm that no oxidation of the flakes has occurred during processing. We have performed X-ray photoelectron spectroscopy on thin films of graphene flakes as shown in Figure 1H. The spectrum is dominated by the C−C peak. While some very small additional peaks are observed between 385 and 287 eV, these are associated with residual solvent.

This data makes it clear that solvents with the correct surface energy can exfoliate graphite to give reasonable quantities of high-quality defect-free graphene. However, surface energy is not an ideal predictor of solvent quality, that is, not all solvents with surface energy close to 68 mJ/m^2 exfoliate graphene. The reason for this is that surface energy is a rather unsophisticated solubility parameter. More useful are the Hansen solubility parameters.[30] These are known to describe the dispersion of nanotubes well[21] suggesting them to be appropriate for use with graphene dispersions. The Hansen solubility parameters are the square roots of the dispersive, polar, and hydrogen bonding components of the cohesive energy density of a material and are denoted δ_D, δ_P, and δ_H, respectively. Hansen has suggested that the enthalpy of mixing is given by[30]

$$\frac{\Delta H_{Mix}}{V} \approx \left[(\delta_{D,S} - \delta_{D,G})^2 + (\delta_{P,S} - \delta_{P,G})^2/4 + (\delta_{H,S} - \delta_{H,G})^2/4\right]\phi_G \quad (6)$$

where the subscripts S and G represent solvent and graphene, respectively. Substituting this expression into 2 gives an equation for the dispersed concentration, C_G:

$$C_G \propto \exp\left[-\frac{\overline{V}_G}{RT}(\delta_{D,S} - \delta_{D,G})^2\right] \exp\left[-\frac{\overline{V}_G}{RT}(\delta_{P,S} - \delta_{P,G})^2/4\right] x \exp\left[-\frac{\overline{V}_G}{RT}(\delta_{H,S} - \delta_{H,G})^2/4\right] \quad (7)$$

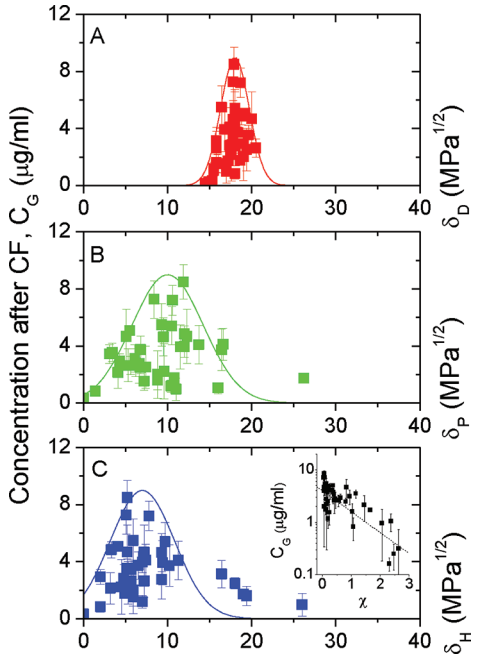

FIGURE 2. Dispersed graphene concentration as a function of (A) dispersive, (B) polar, and (C) hydrogen bonding Hansen solubility parameters. Inset shows log of dispersed concentration as a function of Flory–Huggins parameter. Linearity (dashed line) is expected from solubility theory. Note all solvents included in this data set are listed in the Supporting Information.

where $\bar{v}_G$ is the graphene molar mass. This predicts that the dispersed concentration is maximized in solvents where all Hansen parameters match those of graphene. This is shown to be the case in Figure 2,[31] which shows well-defined peaks bounded by Gaussian functions (eq 7). These data suggest that graphene is described by Hansen parameters of $\delta_{D,G} \approx 18$ MPa$^{1/2}$, $\delta_{P,G} \approx 10$ MPa$^{1/2}$,and $\delta_{H,G} \approx 7$ MPa$^{1/2}$.

We note that eq 7 can be abbreviated to

$$C_G = \exp[\bar{v}_G\chi/\bar{v}_S] \quad (8)$$

where $\bar{v}_S$ is the solvent molar mass and χ is the Flory–Huggins parameter. This parameter can be estimated from the graphene and solvent Hansen parameters (eqs 7 and 8) and is often used to discuss the energetics of polymer solutions. Equation 8 predicts that ln C_G should fall linearly with χ. The inset in Figure 2 shows this predicted behavior, supporting the idea that solution thermodynamics can be used as a framework to describe graphene–solvent mixtures. It is worth noting that during this work,[31] early analysis of the data for a subset of solvents suggested approximate Hansen parameters for graphene. This allowed us to search for new solvents with Hansen parameters in this region. This approach resulted in the discovery of a number of new solvents for graphene. However, it is worth emphasizing that this does not mean that the analysis described above is a complete description of the dispersion process. It is doubtful whether the combination of dispersive, polar, and H-bonding interactions accurately describes the system at the molecular scale. More work is required to fully understand graphene–solvent interactions.

The concentrations shown in Figures 1A and 2 are too low to be useful for many applications. We attempted to increase the dispersed concentration by optimizing the processing parameters, notably the sonication time. We prepared dispersions of graphene in NMP that were bath-sonicated for a range of times from 0.5 to ~400 h.[26] Using absorption spectroscopy to measure the dispersed concentration after centrifugation, we found C_G to increase from 0.05 to >1 mg/mL (Figure 3A). Interestingly, this graph showed C_G to scale very well with the square root of sonication time: $C_G \propto \sqrt{t}$. TEM characterization showed the flakes to appear of good quality, even after long sonication times, with on average ~3 monolayers per flake for all sonication times. However, the mean flake length, $\langle L \rangle$, and width, $\langle w \rangle$, were observed to fall as $t^{-1/2}$ as predicted for sonication-induced scission.[32] Detailed analysis shows that this time-dependence leads to the observed $C_G \propto \sqrt{t}$ behavior.[26]

It is worth considering whether the long sonication induces basal plane defects. While Raman spectra of films deposited from the dispersed graphene showed a D band, it is very small compared with defective graphene-like materials.[17] This suggests the D band measured here to be associated with flake edges. Were this the case, the average ratio of Raman D to G bands should scale as the flake edge to area ratio: $\langle I_D/I_G \rangle \propto [\langle L \rangle^{-1} + \langle w \rangle^{-1}]$. We measured this ratio and the mean flake length and width using TEM.[26] As shown in Figure 3B, we see very good agreement with this prediction. This confirms that the Raman data is entirely consistent with the production of edges by sonication, suggesting that the flakes are largely free of point defects. In addition, by fitting the data, we found that

$$\langle I_D/I_G \rangle(t) - (I_D/I_G)_{powder} = \Delta I_D/I_G = 0.065[\langle L \rangle^{-1} + \langle w \rangle^{-1}] \quad (9)$$

where the dimensions are measured in micrometers.[26] From the TEM analysis, we know that $\langle L/w \rangle \approx 3$, allowing us to approximate $\Delta I_D/I_G \approx 0.26/\langle L \rangle$. This expression can be used to estimate the size of flakes from Raman measurements.

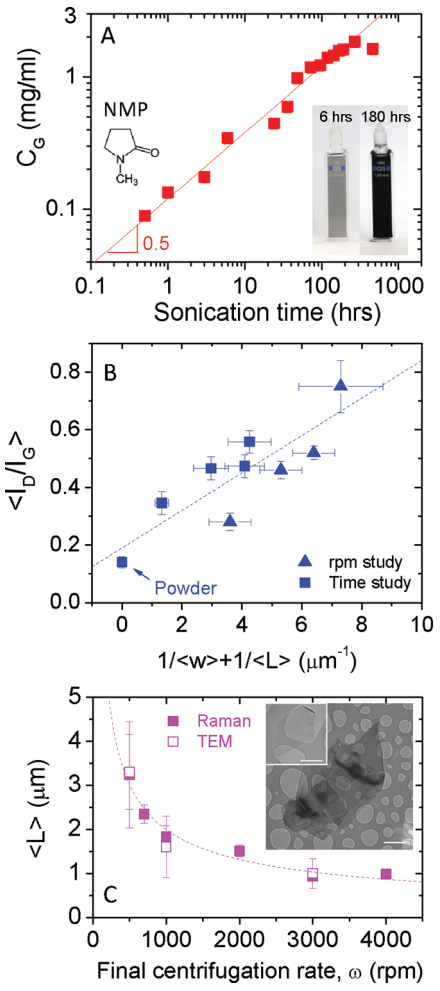

FIGURE 3. (A) Concentration of dispersed graphene in *N*-methyl-pyrrolidone as a function of sonication time. The line illustrates square root behavior. Insets show photos of dispersions after two different sonication times and the structure of the solvent. (B) Defect content as represented by the Raman D/G ratio plotted versus flake length to area ratio. (C) Length of size-selected flakes plotted as a function of final centrifugation rate. Inset shows flakes found after final centrifugation at 3000 rpm (small flake) and 5000 rpm (large flakes). In each case, the scales are identical; scale bar = 500 nm.

While concentrations of ~1 mg/mL can be achieved by long sonication, it would be useful to push this even higher if possible. We found that if a graphene dispersion, prepared as described above, is filtered through a membrane to give a film, it retains the Raman spectrum of few layer flakes[29] rather than reaggregating to graphite.[26] This suggests that within the film, the flakes are weakly interacting and so should be easy to redisperse. We found this to be the case; sonication of such restacked films gave dispersed concentrations of up to 60 mg/mL.[33] While these dispersions were unstable, we found that ~25 mg/mL remained dispersed indefinitely.

Another problem with solvent-dispersed graphene is that the flake length is typically <1 μm, too small for many applications such as mechanical reinforcement of composites.[34] To address this, we attempted to select flakes by size, separating large from small.[41] By centrifuging a high concentration dispersion at 4000 rpm, we separated the smallest flakes into the supernatant from the larger ones in the sediment. The sediment was redispersed and centrifuged at 3000 rpm. This again separated smaller (supernatant) from larger flakes (sediment). This procedure was repeated a number of times until a centrifugation rate of 500 rpm was reached. We characterized the flake size in each supernatant by TEM and using Raman spectroscopy. We round the flake size to increase from ~1 μm for the 4000 rpm sample to ~3 μm for the 500 rpm sample (Figure 3C). This method is both practical and effective and is now in standard usage in our laboratory to prepare dispersions of relatively large flakes.

A final problem with our approach to dispersing graphene is that solvents that have the correct surface energy to disperse graphene also have high boiling points, causing practical difficulties. By examining the data in Figure 2 more closely, we identified a small number of solvents, notably isopropanol and acetone, with relatively low boiling points. Unfortunately, they dispersed graphene at concentrations much lower than the better solvents. To address this, we used the approach described above of increasing the sonication time,[35] reaching concentrations as high as 0.5 mg/mL after 300 h. As with other solvents, the flakes were defect free. Using low boiling point solvents brings considerable advantages; for example, spray-casting of individual multilayer graphene flakes on surfaces was greatly simplified by using isopropanol.

We are currently working to scaleup solvent exfoliation of graphene. We now routinely produce up to a liter of graphene dispersion containing ~1 g of graphene.

It is worth noting that a number of other groups have made considerable progress toward exfoliating graphene in solvents.[36−47] This work has contributed greatly to our understanding of the dispersion process, our practical approach to dispersion, and the number of solvents available to graphene researchers.

Surfactant Stabilization of Graphene. For many applications, exfoliation of graphene in solvents is undesirable due to a number of issues such as high boiling point, toxicity, incompatibility with other aspects of processing, etc. To address this, we studied the possibility of exfoliating graphene in water in the presence of a surfactant stabilizer. We found that graphene can indeed be exfoliated by sonicating in aqueous solutions of surfactants such as

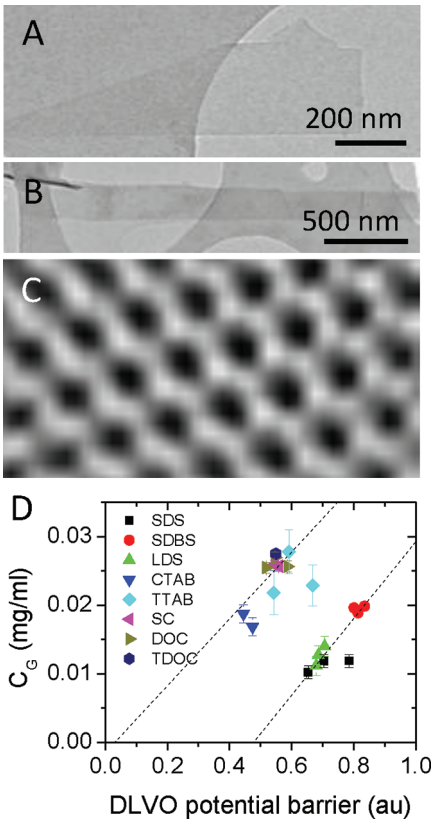

FIGURE 4. (A, B) TEM images of surfactant-exfoliated flakes. (C) Digitally filtered high-resolution image of a surfactant-exfoliated flake. (D) Dispersed concentration as a function of electrostatic potential barrier. The full names and structures of the surfactants are given in the Supporting Information.

sodium dodecylbenzenesulfonate and sodium cholate (Figure 4A–C)). Although the fraction of monolayers is not as high as for solvent-exfoliated graphene, the flake quality is good with little evidence of defects or oxides.[48,49] As is the case for solvent exfoliation, the concentration can be increased dramatically by increasing the sonication time, approaching 0.3 mg/mL for 400 h sonication.[49] However, it is worth noting that the flake size does not decrease with sonication time as much as is observed for solvent exfoliation. This may be due to poor stress transfer during cavitation at the water/surfactant/graphene interface.

Like many colloidal systems, surfactant-coated graphene is stabilized electrostatically against aggregation. Dissociation of the headgroup ions results in the formation of an electrical double-layer.[50] The resultant Coulomb repulsion stabilizes the sheets and is generally characterized by the ζ potential, the electrical potential at the edge of the layer of bound surfactant molecular ions. We studied a range of surfactants as stabilizers, finding ζ potentials in the range $\pm$25–65 mV.[51] More interestingly, we found the dispersed concentration to scale with the square of the ζ potential.

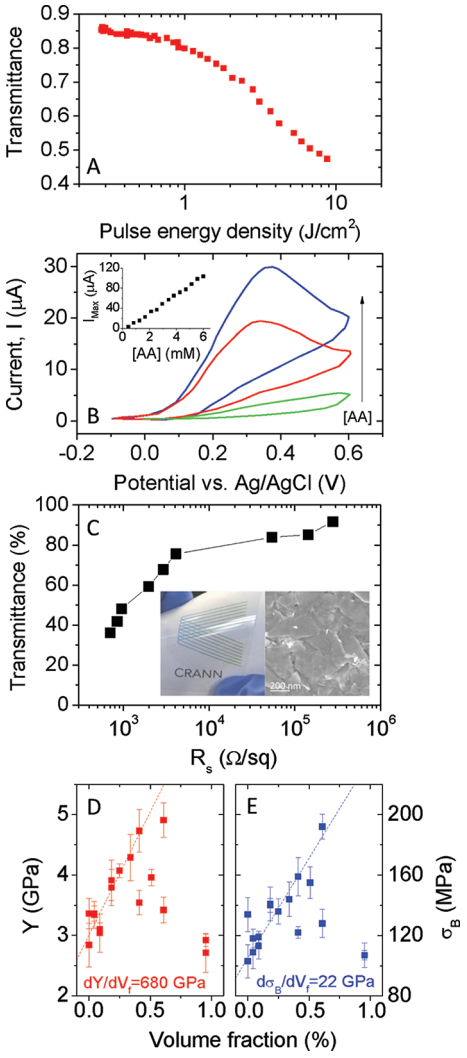

FIGURE 5. (A) Measured transmittance as a function of pulse energy density for a dispersion of graphene in dimethylacetamide. (B) Cyclic voltammograms of graphene electrodes in ascorbic acid (AA) solutions at a range of concentrations. Inset shows the electrocatalytic peak current against ascorbic acid concentration. (C) Transmittance versus sheet resistance for graphene thin films. Insets show photograph of a transparent conducting film (left) and SEM image of the film surface (right). (D) Young's modulus and (E) strength of graphene–poly(vinyl alcohol) composites as a function of graphene volume fraction. The slopes of the linear regions are given.

Because the electrostatic repulsive barrier stabilizing the surfactant-coated graphene also scales approximately with the square of the ζ potential,[48] this suggests that the dispersed concentration is controlled by the size of this repulsive barrier (Figure 4D).

It is worth noting that much progress has been made in surfactant exfoliation outside our group.[52–56] This has led to a number of advances including using density gradient centrifugation to separate graphene flakes by thickness.[52] In addition, it was recently shown that graphene can be

exfoliated using adsorbed polymer as a stabilizer.[57] Here the stabilization mechanism is steric[50] rather than electrostatic. We extended this method to show that graphene can be stabilized with polyurethane and poly(vinyl alcohol), a procedure that greatly facilitates composite formation.[58,59]

Applications of Liquid-Exfoliated Graphene. In our group, we have explored using solvent- or surfactant-exfoliated graphene in a number of applications. We have found that dispersions of graphene in solvents display a considerable broadband nonlinear optical response when excited by nanosecond pulses.[60] The optical transmission of ~85% transparent dispersions falls to ~48% as the pulse energy density is increased to 10 J/cm^2, suggesting the potential for optical limiting applications (Figure 5A).

We have also shown that pristine solvent-exfoliated graphene shows potential as an electrode material in electrochemical sensors.[42] We produced a novel ascorbic acid sensor based on pyrolyzed photoresist films coated with graphene. This sensor was effective in the range 0.4−6.0 mM, with a 0.12 mM detection limit (Figure 5B). We extended this work to demonstrate sensing of β-nicotinamide adenine dinucleotide (NADH), a common enzyme.[61] This works because the fouling that commonly hampers carbon-based NADH sensors does not occur at the pristine graphene surface.

We also attempted to prepare high-performance transparent conductors from vacuum-filtered films of surfactant-exfoliated graphene. However the results were disappointing; we achieved no better than transmittance of 76% coupled with a sheet resistance of 4 kΩ,[62] far below state-of-the-art materials (Figure 5C).[63] This prompted us to reanalyze a large number of published works, leading to the conclusion that the effect of interflake junction resistances means that films of liquid-exfoliated graphene can never meet industry requirements for transparent conducting electrodes.[64] They may however, be useful in applications where transparency is required but extremely low resistance is not necessary. However, we were able to show that graphene can be mixed with nanotubes to create hybrid films.[65] These films have combinations of transmittance and sheet resistance significantly better than films of nanotubes or graphene alone.[66]

Due to its extremely high strength,[10] one of the most promising applications of graphene is as a reinforcing material in polymer-based composites. We found that as-prepared liquid-exfoliated graphene can be used to effectively increase the low-strain−stress of elastomers[58] but was less effective at reinforcing thermoplastics. We resolved this by using the size-selection technique described above to prepare dispersions of large aspect ratio flakes, which could be mixed with poly(vinyl alcohol) to give composites. We found very good reinforcement as characterized by a doubling in both modulus and strength on addition of <0.5 wt % graphene (Figure 5D).[59] Detailed analysis showed these results to be exactly what would be expected from theory.

Beyond Graphene. A number of groups have shown that graphene can be chemically modified to produce compounds such as CF_x and CH_x.[67−69] However, one can go beyond carbon altogether. Graphite is just one of a wide range of layered compounds. Exfoliation of such materials would give us a large number of new two-dimensional materials with a wide range of properties. The first progress was reported recently with the solvent exfoliation of boron nitride.[70] Perhaps more interesting is the family of transition metal dichalcogenides, which contains over 40 members with compositions such as MoS_2, WSe_2, $NiTe_2$, etc. These materials can be metallic or semiconducting with a range of bandgaps depending on composition. Recently, we showed that a range of these materials can be exfoliated in large quantities either in solvents or using surfactants.[71] Importantly, dispersions of these materials can be mixed with dispersions of nanotubes or graphene to produce highly conductive hybrids. We anticipate that these hybrids will be useful in a range of areas from Li ion batteries to thermoelectrics.

Concluding Remarks

As the potential applications of graphene multiply, it will become more and more important to be able to produce defect-free graphene in large quantities. In this report, we have shown that this can be achieved by sonication of graphite in certain liquids. The ultrasound results in the exfoliation and cutting of the graphite crystallites to give graphene nanosheets. These sheets are then stabilized, either by interaction with the solvent or by the presence of adsorbed surfactant or polymer. Raman and XPS spectroscopies show the flakes to be defect- and oxide-free. While we have shown these flakes to be useful in a number of applications, we believe the next decade will see an explosion in the usage of these materials in a wide range of applications.

I would like to acknowledgment SFI funding under the PI award scheme, Contract Number 07/IN.1/I1772. In addition, I must thank all those within my group who contributed to this work. It is impossible to mention you all, but special thanks must go to Dr. Yenny Hernandez and Dr. Valeria Nicolosi.

Supporting Information. List of solvents and surfactants. This material is available free of charge via the Internet at http://pubs.acs.org.

BIOGRAPHICAL INFORMATION

Jonathan Coleman was born in Dublin, Ireland, in 1973. He received both his B.A (1995) and Ph.D. (2000) in Physics from Trinity College Dublin. He remained at Trinity as a postdoctoral researcher, lecturer, and associate professor. He is now Professor of Chemical Physics and a Principal Investigator in the Centre for Research on Adaptive Nanostructures and Nanodevices (CRANN). His research interests focus on the processing of nanomaterials in liquids for a range of applications.

FOOTNOTES

*E-mail: colemaj@tcd.ie.

The authors declare no competing financial interest.

REFERENCES

1 *The Cambridge Ancient History*; Boardman, J., Edwards, I. E. S., Hammond, N. G. L., Sollberger, E., Eds.; Cambridge University Press: Cambridge, U.K., 2008; Vol. 3, Part 1.

2 Bernal, J. D. The Structure of Graphite. *Proc. R. Soc. London, Ser. A* **1924**, *106*, 749–773.

3 Geim, A. K. Graphene: Status and Prospects. *Science* **2009**, *324*, 1530–1534.

4 Geim, A. K.; Novoselov, K. S. The Rise of Graphene. *Nat. Mater.* **2007**, *6*, 183–191.

5 Wallace, P. R. The Band Theory of Graphite. *Phys. Rev.* **1947**, *71*, 622–634.

6 Mermin, N. D. Crystalline Order in Two Dimensions. *Phys. Rev.* **1968**, *176*, 250–254.

7 Boehm, H. P.; Clauss, A.; Fischer, G.; Hofmann, U. Surface properties of extremely thin graphite lamellae. *Proceedings of the Fifth Conference on Carbon*; Pergamon Press: New York, 1962; pp 73−80.

8 Lu, X. K.; Yu, M. F.; Huang, H.; Ruoff, R. S. Tailoring Graphite with the Goal of Achieving Single Sheets. *Nanotechnology* **1999**, *10*, 269–272.

9 Novoselov, K. S.; Geim, A. K.; Morozov, S. V.; Jiang, D.; Zhang, Y.; Dubonos, S. V.; Grigorieva, I. V.; Firsov, A. A. Electric Field Effect in Atomically Thin Carbon Films. *Science* **2004**, *306*, 666–669.

10 Lee, C.; Wei, X. D.; Kysar, J. W.; Hone, J. Measurement of the Elastic Properties and Intrinsic Strength of Monolayer Graphene. *Science* **2008**, *321*, 385–388.

11 Bae, S.; Kim, H.; Lee, Y.; Xu, X. F.; Park, J. S.; Zheng, Y.; Balakrishnan, J.; Lei, T.; Kim, H. R.; Song, Y. I.; Kim, Y. J.; Kim, K. S.; Ozyilmaz, B.; Ahn, J. H.; Hong, B. H.; Iijima, S. Roll-to-Roll Production of 30-in. Graphene Films for Transparent Electrodes. *Nat. Nanotechnol.* **2010**, *5*, 574–578.

12 Berger, C.; Song, Z. M.; Li, X. B.; Wu, X. S.; Brown, N.; Naud, C.; Mayo, D.; Li, T. B.; Hass, J.; Marchenkov, A. N.; Conrad, E. H.; First, P. N.; de Heer, W. A. Electronic Confinement and Coherence in Patterned Epitaxial Graphene. *Science* **2006**, *312*, 1191–1196.

13 Kim, K. S.; Zhao, Y.; Jang, H.; Lee, S. Y.; Kim, J. M.; Kim, K. S.; Ahn, J.-H.; Kim, P.; Choi, J.-Y.; Hong, B. H. Large-Scale Pattern Growth of Graphene Films for Stretchable Transparent Electrodes. *Nature* **2009**, *457*, 706–710.

14 Li, X. S.; Cai, W. W.; An, J. H.; Kim, S.; Nah, J.; Yang, D. X.; Piner, R.; Velamakanni, A.; Jung, I.; Tutuc, E.; Banerjee, S. K.; Colombo, L.; Ruoff, R. S. Large-Area Synthesis of High-Quality and Uniform Graphene Films on Copper Foils. *Science* **2009**, *324*, 1312–1314.

15 Kuilla, T.; Bhadra, S.; Yao, D. H.; Kim, N. H.; Bose, S.; Lee, J. H. Recent Advances in Graphene Based Polymer Composites. *Prog. Polym. Sci.* **2010**, *35*, 1350–1375.

16 Ruoff, R. Calling All Chemists. *Nat. Nanotechnol.* **2008**, *3*, 10–11.

17 Stankovich, S.; Dikin, D. A.; Piner, R. D.; Kohlhaas, K. A.; Kleinhammes, A.; Jia, Y.; Wu, Y.; Nguyen, S. T.; Ruoff, R. S. Synthesis of Graphene-Based Nanosheets via Chemical Reduction of Exfoliated Graphite Oxide. *Carbon* **2007**, *45*, 1558–1565.

18 Zhu, Y. W.; Murali, S.; Cai, W. W.; Li, X. S.; Suk, J. W.; Potts, J. R.; Ruoff, R. S. Graphene and Graphene Oxide: Synthesis, Properties, and Applications. *Adv. Mater.* **2010**, *22*, 3906–3924.

19 Coleman, J. N. Liquid-Phase Exfoliation of Nanotubes and Graphene. *Adv. Funct. Mater.* **2009**, *19*, 3680–3695.

20 Bergin, S. D.; Nicolosi, V.; Streich, P. V.; Giordani, S.; Sun, Z. Y.; Windle, A. H.; Ryan, P.; Niraj, N. P. P; Wang, Z. T. T.; Carpenter, L.; Blau, W. J.; Boland, J. J.; Hamilton, J. P.; Coleman, J. N. Towards Solutions of Single-Walled Carbon Nanotubes in Common Solvents. *Adv. Mater.* **2008**, *20*, 1876–1881.

21 Bergin, S. D.; Sun, Z. Y.; Rickard, D.; Streich, P. V.; Hamilton, J. P.; Coleman, J. N. Multicompenent Solubility Parameters for Single Walled Carbon Nanotube−Solvent Mixtures. *ACS Nano* **2009**, *3*, 2340–2350.

22 Hughes, J. M.; Aherne, D.; Bergin, S. D.; Streich, P. V.; Hamilton, J. P.; Coleman, J. N. Using Solution Thermodynamics to Describe the Dispersion of Carbon Nanotubes in Organic Solvents. *Langmuir* **2011**, *in press*.

23 Hernandez, Y.; Nicolosi, V.; Lotya, M.; Blighe, F. M.; Sun, Z. Y.; De, S.; McGovern, I. T.; Holland, B.; Byrne, M.; Gun'ko, Y. K.; Boland, J. J.; Niraj, P.; Duesberg, G.; Krishnamurthy, S.; Goodhue, R.; Hutchison, J.; Scardaci, V.; Ferrari, A. C.; Coleman, J. N. High-Yield Production of Graphene by Liquid-Phase Exfoliation of Graphite. *Nat. Nanotechnol.* **2008**, *3*, 563–568.

24 Lyklema, J. The Surface Tension of Pure Liquids - Thermodynamic Components and Corresponding States. *Colloids Surf., A* **1999**, *156*, 413–421.

25 Wang, S. R.; Zhang, Y.; Abidi, N.; Cabrales, L. Wettability and Surface Free Energy of Graphene Films. *Langmuir* **2009**, *25*, 11078–11081.

26 Khan, U.; O'Neill, A.; Lotya, M.; De, S.; Coleman, J. N. High-Concentration Solvent Exfoliation of Graphene. *Small* **2010**, *6*, 864–871.

27 Meyer, J. C.; Geim, A. K.; Katsnelson, M. I.; Novoselov, K. S.; Obergfell, D.; Roth, S.; Girit, C.; Zettl, A. On the Roughness of Single- And Bi-layer Graphene Membranes. *Solid State Commun.* **2007**, *143*, 101–109.

28 Horiuchi, S.; Gotou, T.; Fujiwara, M.; Sotoaka, R.; Hirata, M.; Kimoto, K.; Asaka, T.; Yokosawa, T.; Matsui, Y.; Watanabe, K.; Sekita, M. Carbon Nanofilm with a New Structure and Property. *Jpn. J. Appl. Phys., Part 2* **2003**, *42*, L1073–L1076.

29 Ferrari, A. C.; Meyer, J. C.; Scardaci, V.; Casiraghi, C.; Lazzeri, M.; Mauri, F.; Piscanec, S.; Jiang, D.; Novoselov, K. S.; Roth, S.; Geim, A. K. Raman Spectrum of Graphene and Graphene Layers. *Phys. Rev. Lett.* **2006**, *97*, No. 187401.

30 Hansen, C. M. *Hansen Solubility Parameters - A User's Handbook*; CRC Press: Boca Raton, FL, 2007.

31 Hernandez, Y.; Lotya, M.; Rickard, D.; Bergin, S. D.; Coleman, J. N. Measurement of Multicomponent Solubility Parameters for Graphene Facilitates Solvent Discovery. *Langmuir* **2010**, *26*, 3208–3213.

32 Hennrich, F.; Krupke, R.; Arnold, K.; Rojas Stutz, J. A.; Lebedkin, S.; Koch, T.; Schimmel, T.; Kappes, M. M. The Mechanism of Cavitation-Induced Scission of Single-Walled Carbon Nanotubes. *J. Phys. Chem. B* **2007**, *111*, 1932–1937.

33 Khan, U.; Porwal, H.; O'Neill, A.; Nawaz, K.; May, P.; Coleman, J. N. Solvent-Exfoliated Graphene at Extremely High Concentration. *Langmuir* **2011**, *27*, 9077–9082.

34 Gong, L.; Kinloch, I. A.; Young, R. J.; Riaz, I.; Jalil, R.; Novoselov, K. S. Interfacial Stress Transfer in a Graphene Monolayer Nanocomposite. *Adv. Mater.* **2010**, *22*, 2694–2697.

35 O'Neill, A.; Khan, U.; Nirmalraj, P. N.; Boland, J. J.; Coleman, J. N. Graphene Dispersion and Exfoliation in Low Boiling Point Solvents. *J. Phys. Chem. C* **2011**, *115*, 5422–5428.

36 Blake, P.; Brimicombe, P. D.; Nair, R. R.; Booth, T. J.; Jiang, D.; Schedin, F.; Ponomarenko, L. A.; Morozov, S. V.; Gleeson, H. n. F.; Hill, E. W.; Geim, A. K.; Novoselov, K. S. Graphene-Based Liquid Crystal Device. *Nano Lett.* **2008**, *8*, 1704–1708.

37 Bourlinos, A. B.; Georgakilas, V.; Zboril, R.; Steriotis, T. A.; Stubos, A. K. Liquid-Phase Exfoliation of Graphite Towards Solubilized Graphenes. *Small* **2009**, *5*, 1841–1845.

38 Hamilton, C. E.; Lomeda, J. R.; Sun, Z. Z.; Tour, J. M.; Barron, A. R. High-Yield Organic Dispersions of Unfunctionalized Graphene. *Nano Lett.* **2009**, *9*, 3460–3462.

39 Hasan, T.; Torrisi, F.; Sun, Z.; Popa, D.; Nicolosi, V.; Privitera, G.; Bonaccorso, F.; Ferrari, A. C. Solution-Phase Exfoliation of Graphite for Ultrafast Photonics. *Phys. Status Solidi B* **2010**, *247*, 2953–2957.

40 Choi, E. Y.; Choi, W. S.; Lee, Y. B.; Noh, Y. Y. Production of Graphene by Exfoliation of Graphite in a Volatile Organic Solvent. *Nanotechnology* **2011**, *22*, No. 365601.

41 Khan, U.; O'Neill, A.; Porwal, H.; May, P.; Nawaz, K.; Coleman, J. N. Size Selection of Dispersed, Exfoliated Graphene Flakes by Controlled Centrifugation. *Carbon* **2012**, *50*, 470–475.

42 Keeley, G. P.; O'Neill, A.; McEvoy, N.; Peltekis, N.; Coleman, J. N.; Duesberg, G. S. Electrochemical Ascorbic Acid Sensor Based on DMF-Exfoliated Graphene. *J. Mater. Chem.* **2010**, *20*, 7864–7869.

43 Liang, Y. T.; Hersam, M. C. Highly Concentrated Graphene Solutions via Polymer Enhanced Solvent Exfoliation and Iterative Solvent Exchange. *J. Am. Chem. Soc.* **2010**, *132*, 17661–17663.

44 Nuvoli, D.; Valentini, L.; Alzari, V.; Scognamillo, S.; Bon, S. B.; Piccinini, M.; Illescas, J.; Mariani, A. High Concentration Few-Layer Graphene Sheets Obtained by Liquid Phase Exfoliation of Graphite in Ionic Liquid. *J. Mater. Chem.* **2011**, *21*, 3428–3431.

45 Zhang, X. Y.; Coleman, A. C.; Katsonis, N.; Browne, W. R.; van Wees, B. J.; Feringa, B. L. Dispersion of Graphene in Ethanol Using a Simple Solvent Exchange Method. *Chem. Commun.* **2010**, *46*, 7539–7541.

46 Alzari, V.; Nuvoli, D.; Scognamillo, S.; Piccinini, M.; Gioffredi, E.; Malucelli, G.; Marceddu, S.; Sechi, M.; Sanna, V.; Mariani, A. Graphene-Containing Thermoresponsive Nanocomposite Hydrogels of Poly(N-isopropylacrylamide) Prepared by Frontal Polymerization. *J. Mater. Chem.* **2011**, *21*, 8727–8733.

47 Shih, C. J.; Lin, S. C.; Strano, M. S.; Blankschtein, D. Understanding the Stabilization of Liquid-Phase-Exfoliated Graphene in Polar Solvents: Molecular Dynamics Simulations and Kinetic Theory of Colloid Aggregation. *J. Am. Chem. Soc.* **2010**, *132*, 14638–14648.

48 Lotya, M.; Hernandez, Y.; King, P. J.; Smith, R. J.; Nicolosi, V.; Karlsson, L. S.; Blighe, F. M.; De, S.; Wang, Z.; McGovern, I. T.; Duesberg, G. S.; Coleman, J. N. Liquid Phase Production of Graphene by Exfoliation of Graphite in Surfactant/Water Solutions. *J. Am. Chem. Soc.* **2009**, *131*, 3611–3620.

49 Lotya, M.; King, P. J.; Khan, U.; De, S.; Coleman, J. N. High-Concentration, Surfactant-Stabilized Graphene Dispersions. *ACS Nano* **2010**, *4*, 3155–3162.

50 Israelachvili, J. *Intermolecular and Surface Forces*; 2nd ed.; Academic Press: London, 1991.

51 Smith, R. J.; Lotya, M.; Coleman, J. N. The Importance of Repulsive Potential Barriers for the Dispersion of Graphene Using Surfactants. *New J. Phys.* **2010**, *12*, No. 125008.

52 Green, A. A.; Hersam, M. C. Solution Phase Production of Graphene with Controlled Thickness via Density Differentiation. *Nano Lett.* **2009**, *9*, 12–17.

53 Hao, R.; Qian, W.; Zhang, L. H.; Hou, Y. L. Aqueous Dispersions of TCNQ-Anion-Stabilized Graphene Sheets. *Chem. Commun.* **2008**, 6576–6578.

54 Vadukumpully, S.; Paul, J.; Valiyaveettil, S. Cationic Surfactant Mediated Exfoliation of Graphite into Graphene Flakes. *Carbon* **2009**, *47*, 3288–3294.

55 Lin, S. C.; Shih, C. J.; Strano, M. S.; Blankschtein, D. Molecular Insights into the Surface Morphology, Layering Structure, and Aggregation Kinetics of Surfactant-Stabilized Graphene Dispersions. *J. Am. Chem. Soc.* **2011**, *133*, 12810–12823.

56 Wei, W.; Lu, W.; Yang, Q. H. High-Concentration Graphene Aqueous Suspension and a Membrane Self-Assembled at the Liquid-Air Interface. *New Carbon Mater.* **2011**, *26*, 36–40.

57 Bourlinos, A. B.; Georgakilas, V.; Zboril, R.; Steriotis, T. A.; Stubos, A. K.; Trapalis, C. Aqueous-Phase Exfoliation of Graphite in the Presence of Polyvinylpyrrolidone for the Production of Water-Soluble Graphenes. *Solid State Commun.* **2009**, *149*, 2172–2176.

58 Khan, U.; May, P.; O'Neill, A.; Coleman, J. N. Development of Stiff, Strong, Yet Tough Composites by the Addition of Solvent Exfoliated Graphene to Polyurethane. *Carbon* **2010**, *48*, 4035–4041.

59 May, P.; Khan, U.; O'Neill, A.; Coleman, J. N. Approaching the Theoretical Limit for Reinforcing Polymers with Graphene. *J. Mater. Chem.* **2012**, *22*, 1278–1282.

60 Wang, J.; Hernandez, Y.; Lotya, M.; Coleman, J. N.; Blau, W. J. Broadband Nonlinear Optical Response of Graphene Dispersions. *Adv. Mater.* **2009**, *21*, 2430–2435.

61 Keeley, G. P.; O'Neill, A.; Holzinger, M.; Cosnier, S.; Coleman, J. N.; Duesberg, G. S. DMF-Exfoliated Graphene for Electrochemical NADH Detection. *Phys. Chem. Chem. Phys.* **2011**, *13*, 7747–7750.

62 De, S.; King, P. J.; Lotya, M.; O'Neill, A.; Doherty, E. M.; Hernandez, Y.; Duesberg, G. S.; Coleman, J. N. Flexible, Transparent, Conducting Films of Randomly Stacked Graphene from Surfactant-Stabilized, Oxide-Free Graphene Dispersions. *Small* **2010**, *6*, 458–464.

63 Scardaci, V.; Coull, R.; Lyons, P. E.; Rickard, D.; Coleman, J. N. Spray Deposition of Highly Transparent, Low-Resistance Networks of Silver Nanowires over Large Areas. *Small* **2011**, *7*, 2621–2628.

64 De, S.; Coleman, J. N. Are There Fundamental Limitations on the Sheet Resistance and Transmittance of Thin Graphene Films? *ACS Nano* **2010**, *4*, 2713–2720.

65 Khan, U.; O'Connor, I.; Gun'ko, Y. K.; Coleman, J. N. The Preparation of Hybrid Films of Carbon Nanotubes and Nano-Graphite/Graphene with Excellent Mechanical and Electrical Properties. *Carbon* **2010**, *48*, 2825–2830.

66 King, P. J.; Khan, U.; Lotya, M.; De, S.; Coleman, J. N. Improvement of Transparent Conducting Nanotube Films by Addition of Small Quantities of Graphene. *ACS Nano* **2010**, *4*, 4238–4246.

67 Nair, R. R.; Ren, W. C.; Jalil, R.; Riaz, I.; Kravets, V. G.; Britnell, L.; Blake, P.; Schedin, F.; Mayorov, A. S.; Yuan, S. J.; Katsnelson, M. I.; Cheng, H. M.; Strupinski, W.; Bulusheva, L. G.; Okotrub, A. V.; Grigorieva, I. V.; Grigorenko, A. N.; Novoselov, K. S.; Geim, A. K. Fluorographene: A Two-Dimensional Counterpart of Teflon. *Small* **2010**, *6*, 2877–2884.

68 Zboril, R.; Karlicky, F.; Bourlinos, A. B.; Steriotis, T. A.; Stubos, A. K.; Georgakilas, V.; Safarova, K.; Jancik, D.; Trapalis, C.; Otyepka, M. Graphene Fluoride: A Stable Stoichiometric Graphene Derivative and Its Chemical Conversion to Graphene. *Small* **2010**, *6*, 2885–2891.

69 Elias, D. C.; Nair, R. R.; Mohiuddin, T. M. G.; Morozov, S. V.; Blake, P.; Halsall, M. P.; Ferrari, A. C.; Boukhvalov, D. W.; Katsnelson, M. I.; Geim, A. K.; Novoselov, K. S. Control of Graphene's Properties by Reversible Hydrogenation: Evidence for Graphane. *Science* **2009**, *323*, 610–613.

70 Zhi, C. Y.; Bando, Y.; Tang, C. C.; Kuwahara, H.; Golberg, D. Large-Scale Fabrication of Boron Nitride Nanosheets and Their Utilization in Polymeric Composites with Improved Thermal and Mechanical Properties. *Adv. Mater.* **2009**, *21*, 2889–2893.

71 Smith, R. J.; King, P. J.; Lotya, M.; Wirtz, C.; Khan, U.; De, S.; O'Neill, A.; Duesberg, G. S.; Grunlan, J. C.; Moriarty, G.; Chen, J.; Wang, J. Z.; Minett, A. I.; Nicolosi, V.; Coleman, J. N. Large-Scale Exfoliation of Inorganic Layered Compounds in Aqueous Surfactant Solutions. *Adv. Mater.* **2011**, *23*, 3944–3948.